ANALYSIS OF MASS TRANSFER CAPACITY IN RACEWAY REACTORS

M. Barceló-Villalobos[1], J. L. Guzmán Sánchez [1], I. Martín Cara[2], J.A. Sánchez Molina[1] F. G. Acién Fernández[2*]

[1]Department of Informatics, Universidad de Almería, E04120 Almería (Spain)

[2]Department of Chemical Engineering, Universidad de Almería, E04120 Almería (Spain)

*Corresponding author. E-mail address: mbarcelovillalobos@gmail.com (M. Barceló-Villalobos)

Keywords: Microalgae, raceways, mass transfer, CO_2 transfer, oxygen desorption

Abstract

In the present work, a methodology is proposed to determine the mass transfer capacity in existing microalgae raceway reactors to minimize excessive dissolved oxygen accumulation that would otherwise reduce biomass productivity. The methodology has been validated using a 100 m^2 raceway reactor operated in semi-continuous mode. The relevance of each raceway reactor section was evaluated as well as the oxygen transfer capacity in the sump to different air flow rates. The results confirm that dissolved oxygen accumulates in raceway reactors if no appropriate mass transfer systems are provided. Therefore, mass transfer in the sump is the main contributor to oxygen removal in these systems. The variation in the volumetric mass transfer coefficient in the sump as a function of the gas flow rate, and therefore the superficial gas velocity in the sump, has been studied and modelled. Moreover, the developed model has been used to estimate the mass transfer requirements in the sump as a function of the target dissolved oxygen concentration and the oxygen production rate. The proposed methodology allows us to determine and optimize the mass transfer capacity in the sump for any existing raceway reactor. Moreover, it is a powerful tool for the optimization of existing reactors as well as for the design optimization of new reactors.

1. INTRODUCTION

Raceway reactors have been used since the 1950s for the industrial production of microalgae. Today, more than 90% of worldwide microalgae biomass production is carried out using these types of reactors [1]. The major advantage of raceway reactors is their simplicity and low construction cost. However, these reactors have certain problems related to their low productivity, high risk of contamination and poor control of growing conditions, in addition to their low mass transfer capacity. It has been demonstrated that the mass transfer capacity in these reactors is limited and must be improved to allow significantly increased biomass productivity [2]. In this regard, improvements are necessary in the fluid dynamics, the related CO_2 absorption and the oxygen desorption to enhance productivity in these systems [1–3]. Moreover, models are required that allow us to determine the mass transfer capacity and overall performance of these reactors for the scaling-up of any reactor type.

To maximize the performance of any microalgae strain, the culture conditions prevailing inside the reactor must be as close to optimal as possible for that strain. Any deviation from optimal culture conditions in outdoor cultures reduces productivity by more than 50% compared to indoor production, even when using closed tubular photobioreactors. These deviations and losses in productivity are still higher in raceway reactors where there is less control of the culture conditions [4,5]. By providing the most suitable culture conditions possible, we can increase biomass productivity, thus reducing the production costs per biomass unit as well as ensuring efficient and stable biomass production. Concerning CO_2 transfer, some works have been carried out optimizing the utilization of the supplied CO_2 to save costs; this is because CO_2 can contribute up to 30% of the total biomass production cost [6,7]. Nonetheless, much less attention has focused on dissolved oxygen accumulation in the system. It is commonly believed that oxygen is naturally desorbed to the atmosphere without the need for specific desorption systems. However, this is erroneous and the negative effect of dissolved oxygen accumulation on biomass productivity in raceway reactors has already been proven, with values surpassing 300% Sat.

reported [2][9]. In this regard, to ensure that dissolved oxygen accumulation does not diminish biomass productivity in raceway reactors, it is imperative to improve the reactor design as well as the operational conditions, especially the mass transfer capacity.

Although the utilization of raceway reactors for the production of microalgae was first proposed in the 1960's, only recently has its design been revised, both from the fluid-dynamic and mass transfer capacity points of view [3,8–12]. Most of the studies focus on improving fluid dynamics to minimize power consumption, especially in biofuels production, whereas others focus on CO_2 transfer to make more efficient use of this expensive raw material. However, only a few studies have focused on oxygen removal and its improvement. Nonetheless, it was reported that reducing dissolved oxygen below 250 %Sat. by injecting flue gases as a source of CO_2 leads to an increase in biomass productivity above 30% compared to cultures operated with pure CO_2, in which dissolved oxygen increases above 300%Sat [3].Thus, it was concluded that being able to manipulate the mass transfer capacity of raceway reactors in order to maintain the dissolved oxygen content below inhibitory values is a challenge.

In this paper, the mass transfer capacity of a pilot-scale raceway reactor is studied to identify the major phenomena taking place, the oxygen accumulation and the contribution of each reactor section to the mass transfer capacity of the entire reactor. The objective is to be able to fit the mass transfer capacity to that required for the productivity or photosynthesis rate of the specific biomass. To do this, a simple novel methodology has been developed using online dissolved oxygen sensors that do not disturb the reactor's normal operation; these can be used to audit any raceway reactor. The methodology has been validated and utilized to estimate the optimal operating conditions in an existing raceway reactor, making it a useful tool for improving this reactor type.

2. MATERIALS AND METHODS

2.1. Microorganism and culture conditions

The microalgae strain *Scenedesmus almeriensis* (CCAP 276/24) was used. Inoculum for the raceway reactor was produced in a 3.0 m^3 tubular photobioreactor under controlled conditions: at pH =8 and at a temperature ranging from 18 to 22ºC using freshwater and Mann & Myers medium prepared using fertilizers: (0.14 $g \cdot L^{-1}$ $K(PO_4)_2$, 0.18 $g \cdot L^{-1}$ $Mg(SO_4)_2$, 0.9 $g \cdot L^{-1}$ $NaNO_3$, 0.02 $mL \cdot L^{-1}$ Welgro, and 0.02 $g \cdot L^{-1}$ Kalentol) [15]. In addition, $NaHCO_3$ was provided once a week to maintain the medium's alkalinity at the optimum 7 mM.

2.2. Raceway reactor design and operational conditions

The raceway reactor is located at the "Las Palmerillas" Research Centre, 36° 48'N–2° 43'W, part of the Cajamar Foundation (Almería, Spain). The reactor consists of two 50 m long channels (0.46 m high × 1 m wide), both connected by 180° bends at each end, with a 0.59 m^3 sump (0.65 m long × 0.90 m wide × 1 m deep) located 1 m along one of the channels (**¡Error! No se encuentra el origen de la referencia.**) [17]. The pH, temperature and dissolved oxygen in the culture were measured at three different places along the reactor length using appropriate probes (5083 T and 5120, Crison, Barcelona, Spain), connected to an MM44 control-transmitter unit (Crison Instruments, Spain), and data acquisition software (Labview, National Instruments) providing complete monitoring and control of the installation. It was previously confirmed that no vertical or transversal gradients of pH, dissolved oxygen and biomass concentration existed, only longitudinal gradients, so the probes were located in the middle of both the culture depth and the channel. The gas flow rate entering the reactor was measured by a mass flow meter (PFM 725S-F01-F, SMC, Tokyo, Japan). The pH of the culture was controlled at 8.0 by on-demand injection of CO_2, whereas temperature was not controlled; it ranged ±5ºC with respect to the daily mean air temperature, which varied from 12ºC in winter to 28ºC in summer. Air was supplied to the reactor from a blower providing 350 mbar overpressure, through a fine bubble

diffuser AFT2100 (ECOTEC, Spain) providing bubbles with a diameter smaller than 2 mm at the minimum pressure drop; the estimated residence time of the bubbles in the sump ranged from 5 to 10 s [3]. The culture received continuous air injection, regardless of the CO_2 demand. The demand for carbon was supplied by the injection of pure CO_2 using an event-based pH controller at pH 8 [13].The raceway reactor was inoculated and operated in batch mode for one week, after which it was operated in semi-continuous mode at 0.4 day^{-1} at a culture depth of 0.15 m. Only data corresponding to steady-state conditions were used. Evaporation inside the reactor was compensated for by the daily addition of fresh medium.

,

2.3. Experimental design

To study the mass transfer capacity in the raceway reactor, experiments were performed in different seasons (spring, summer, autumn and winter) modifying the gas flow rate into the sump (0, 100, 160, 185, 200 and 350 L min^{-1} so the superficial gas velocity was 0.0, 0.0021, 0.0033, 0.0039, 0.0042, 0.0073 m s^{-1}), and the L/G ratio (0.0, 18.0, 12.0, 9.7, 9, 5.1 $L{\cdot}L^{-1}$), while the culture was operated in semi-continuous mode. In this way, we could study the oxygen produced by photosynthesis as well as that removed in the different parts of the reactor under the different culture conditions imposed (Figure 1). These experiments allowed us to quantify the different phenomena taking place and to measure the mass transfer coefficient as a function of the culture conditions.

The reactor was operated throughout all the tests under the same environmental conditions (solar radiation and temperature) and the same operational conditions (biomass concentration and dilution rate). The mean daily solar radiation was 600 µE m^{-2} s^{-1}, the biomass concentration was 0.39 g L^{-1} and the cells did not present signs of any photosynthetic stress (Quantum Yield =

0.69). Under these conditions, the mean biomass productivity was 0.16 $g \cdot L^{-1} \cdot day^{-1}$, equivalent to 23.4 $g \cdot m^{-2} \cdot day^{-1}$.

2.4. Oxygen mass balance

Oxygen mass balances were performed to study the main phenomena taking place inside the reactor. For this, the dissolved oxygen concentration was measured at three different positions (after the paddlewheel, after the sump and at the end of the loop). The oxygen mass balance allows us to calculate the accumulation of dissolved oxygen as a function of oxygen production and mass transfer in each of these sections. Oxygen is produced by photosynthesis and is therefore modified as a function of the culture conditions, especially by changes in solar radiation outdoors throughout the day. In contrast, the mass transfer capacity is only a function of fluid dynamics and the driving force in the different parts of the reactor; the fluid dynamics remains constant during the day whereas the driving force is measured as a function of the dissolved oxygen concentration entering the culture at the different positions (after the paddlewheel, after the sump and at the end of the loop) throughout the day. Therefore, for any raceway reactor section, the following balance defines the dissolved oxygen concentration (Equation 1).

$$O_{2,inlet} + O_{2,produced} = O_{2,outlet} + O_{2,accumulation} \qquad \textit{Equation 1}$$

We consider that the sump is completely dark, because in this section less than 3% of the total volume have irradiance values above 10 $\mu E \cdot m^{-2} \cdot s^{-1}$, so no photosynthesis takes place. Furthermore, oxygen production in the paddlewheel section can be disregarded; hence the dissolved oxygen mass balance is defined by Equation 2, where PO_2 represents the oxygen production and NO_2 represents the oxygen mass transfer capacity in each of the reactor sections.

$$PO_{2,loop} + NO_{2,loop} + NO_{2,sump} + NO_{2,paddlewheel} = O_{2,accumulation} \qquad \textit{Equation 2}$$

The mass transfer capacity is calculated as a function of the global mass transfer coefficient in each reactor section ($K_l a_l$), multiplied by the driving force. This means that the difference between the dissolved oxygen concentration in the liquid ($[O_2]$) and that in equilibrium with the gas phase (air) ($[O_2^*]$) is calculated using Henry's law and the section volume (V) (Equation 3). The influence of temperature on the solubility of dissolved oxygen was included using Equation 4. In this case, the global mass transfer coefficient refers to the liquid phase, assuming that the main resistance to mass transfer takes place here.

$$NO_2 = K_l a_l([O_2] - [O_2^*])V \qquad \textit{Equation 3}$$

$$[O_2^*] = 12.408 - 0.1658 * T \qquad \textit{Equation 4}$$

It was previously reported that the global mass transfer coefficient in the loop of raceway reactors is very low, at 0.9 h^{-1}, as it is independently constant of the culture conditions [3]. This coefficient can be strongly modified if the liquid velocity is greatly enhanced. However, in raceway reactors, the liquid velocity is adjusted to 0.2 $m \cdot s^{-1}$ to minimize power consumption - for this reason, the value of 0.9 h^{-1} is acceptable as the global mass transfer coefficient in the loop. Moreover, by applying the oxygen mass balance to the loop, it is possible to obtain a "virtual oxygen production sensor" as a function of the dissolved oxygen concentration at the beginning and end of the loop, and the flow of liquid inside the reactor (Q_{liquid}); as defined by Equation 5.

$$PO_{2,loop} = Q_{liquid}\,([O_2]_{outlet} - [O_2]_{inlet})_{loop} - K_l a_{l,loop}([O_2] - [O_2^*])_{loop} V_{loop} \qquad \textit{Equation 5}$$

In addition to this, it has been reported that the global mass transfer coefficient at the paddlewheel is in the 164 h^{-1} range; this remains constant as it is a function of the paddlewheel configuration and the rotation speed, which stay constant despite the solar radiation and the culture conditions imposed on the reactor [3]. Consequently, by knowing the photosynthetic production of oxygen from Equation 5 and the global mass transfer coefficient for the

paddlewheel, the global mass transfer coefficient for the sump can be easily calculated using Equation 8.

$$NO_{2,sump} = O_{2,accumulation} - PO_{2,loop} - NO_{2,loop} - NO_{2,paddlewheel} \quad \textit{Equation 6}$$

$$NO_{2,sump} = K_l a_{l,sump}([O_2] - [O_2^*])_{sump} V_{sump} \quad \textit{Equation 7}$$

$$K_l a_{l,sump}([O_2] - [O_2^*])_{sump} V_{sump} \quad \textit{Equation 8}$$

$$= V_{reactor} \frac{d[O_2]}{dt} - PO_{2,loop} - K_l a_{l,loop}([O_2] - [O_2^*])_{loop} V_{loop}$$

$$- K_l a_{l,paddlewheel}([O_2] - [O_2^*])_{paddlewheel} V_{paddlewheel}$$

In this way, by using only the two dissolved oxygen probes located at the beginning and the end of the loop, it is possible to determine both the photosynthesis rate and the global mass transfer coefficient in the sump from the virtual sensors by applying the detailed equations. Given that the global mass transfer coefficient in the sump can be modified simply by modifying the air gas flow supplied, it is greatly advantageous to be able to measure this coefficient during the reactor's operation. Moreover, calibration curves can be obtained to further adjust the mass transfer capacity in the sump by modifying the air flow rate supplied to it.

2.5 Statistical analysis

The effect of the superficial gas velocity (m s^{-1}) on the volumetric mass transfer coefficient (h^{-1}) was correlated by descriptive statistics (correlation, R^2) in a total of 31 days of assays. Data from the reactors were obtained daily as a total of 1440 samples for each day. The Statistica v.7 program was used to perform the statistical analysis.

3. RESULTS AND DISCUSSION

The negative effect of dissolved oxygen accumulation on the performance of microalgae cultures has been widely reported [14,15]. Dissolved oxygen can damage the cultures or modify the metabolism if values over 250 %Sat. are reached; this is because the photosynthesis rate is exponentially reduced above this value [16,17]. In tubular photobioreactors, the loop length is limited by this phenomenon. It has also been necessary to install adequate bubble column

systems to remove all the oxygen produced by photosynthesis [18,19]. In contrast, in raceway reactors, the dissolved oxygen concentration is usually disregarded even though the same phenomenon occurs. Therefore, the same criteria for design and scale-up need to be applied.

In raceway reactors, oxygen is produced by photosynthesis during the day and consumed by respiration at night, modified by the oxygen concentration equilibrium with the air, of 8.8 $mg \cdot L^{-1}$ (20ºC, 1 atm); this is therefore the driving force for the absorption/desorption of oxygen from or to the air. The results show that the dissolved oxygen concentration in the 100 m^2 raceway reactor varies throughout the day, with different values being observed at the different positions considered (Figure 2). Also, the dissolved oxygen varied from 6.0 $mg \cdot L^{-1}$ (70 %Sat.) at night to 18.0 mg L^{-1} (204 %Sat.) during the daylight period, under the culture conditions imposed. Moreover, these extreme measurements were obtained at the end of the channel whereas the values obtained after the paddlewheel and sump were attenuated compared to those at the end of the loop. From these figures, one can reasonably conclude that the optimal position to locate dissolved oxygen probes in raceway reactors is at the end of the channel or before the paddlewheel, as it is there that the major variations in dissolved oxygen can be determined throughout the whole day.

Data clearly show that during the night the dissolved oxygen concentration is lower than that in equilibrium with the air, meaning a driving force exists for oxygen absorption from the air, whereas during the day the dissolved oxygen concentration is higher than that in equilibrium with the air so a driving force exists for oxygen desorption to the atmosphere. Moreover, the figures demonstrate that oxygen is consumed by the respiration process at night as well as being desorbed to the air, especially in the paddlewheel and sump, where the culture is put into intensive contact with the air (Figure 2). One can also conclude that the respiration rate is higher than the oxygen absorption capacity in the paddlewheel and sump due to equilibrium with the air not being achieved. During the daylight period, the photosynthesis rate is higher, modified

by solar radiation; thus oxygen accumulates in the culture because the reactor's mass transfer capacity is lower than the oxygen production rate resulting from photosynthesis. When analysing the dissolved oxygen values at the different locations, it is clear that the oxygen removal capacity in the paddlewheel is limited so the dissolved oxygen concentration after the paddlewheel is slightly lower than at the end of the channel. Although most of the oxygen is removed in the sump, the dissolved oxygen concentration at this point is lowest during the daylight period. The dissolved oxygen concentration after the sump decreases by 15% compared to the channel at midday (15.28 mg L^{-1} and 17.85 mg L^{-1} respectively). This is because it is a dark zone where air is continually being injected at a constant flow rate of 100 $L \cdot min^{-1}$. These results not only confirm that the mass transfer capacity in the sump is the most relevant but also that it is not sufficient to avoid excessive dissolved oxygen accumulation at noon (6.38 g O_2 min^{-1}).. Therefore, the mass transfer capacity in the reactor must be optimized throughout the day as a function of the culture conditions.

Experimental data on the dissolved oxygen concentration in the culture can be used to estimate the oxygen production rate as well as the mass transfer capacity in the different reactor sections. Hence, using Equation 5, the oxygen production rate in the reactor can be calculated from the dissolved oxygen concentrations at the beginning and the end of the channel; this is a more precise value than that obtained when considering the oxygen transferred in the loop. Figure 3 shows the oxygen transfer in the loop, calculated considering a global mass transfer coefficient value of 0.9 h^{-1} [2]; this is minimal at night (below 0.37 $g \cdot min^{-1}$) due to the low mass transfer coefficient and the driving force during this period. Nonetheless, it is positive because the dissolved oxygen concentration in the culture is lower than that in equilibrium with the air. On the other hand, during the day, the driving force is far greater and the oxygen transfer in the loop is more relevant (-1.74 $g \cdot min^{-1}$ at noon); this is negative (desorption) because the culture is oversaturated with oxygen produced by photosynthesis. If one only considers the variation in dissolved oxygen concentration at the beginning and the end of the channel, a non-valid oxygen

242 production rate is obtained; whereas by considering the oxygen transferred in the channel, the
243 corrected oxygen production rate is a valid measurement. No large deviations in either the non-
244 valid or the corrected oxygen production rates are observed but the net values are slightly
245 different. According to these results, the maximum respiration rate at night was 1.45 $g \cdot min^{-1}$
246 (equivalent to 5.8 $mgO_2 \cdot L^{-1} \cdot h^{-1}$), whereas the maximum oxygen production rate during the
247 daylight period was 6.36 $g \cdot min^{-1}$ (equivalent to 25.4 $mgO_2 \cdot L^{-1} \cdot h^{-1}$). Moreover, a net oxygen
248 amount of 1198 g was produced during the complete daylight period. Therefore, considering a
249 stoichiometric value of 1.33 gO_2 per gram of biomass obtained from the basic photosynthesis
250 equation, we estimated that up to 0.9 kg of biomass would be produced in this reactor under
251 the assayed experimental conditions. However, the net amount of biomass produced was 2.34
252 kg, thus indicating that the basic photosynthesis equation is not completely valid in estimating
253 biomass production outdoors. Thus, due to the existence of other phenomena such as
254 photorespiration, amongst others, the amount of oxygen produced per g of oxygen varies from
255 0.85 to 2.26 $gO_2 \cdot g_{biomass}^{-1}$ [3].

256 In this way, the proposed methodology can estimate the biomass production capacity from the
257 dissolved oxygen measurements. However, the most relevant application is the ability to
258 determine and optimize the mass transfer requirements. Therefore, by applying a mass balance
259 to the paddlewheel, it is possible to estimate the mass transfer in this section; while using
260 Equation 6, it is also possible to determine the mass transfer in the sump, thus obtaining an
261 overall picture of the mass transfer and oxygen production in the entire reactor (Figure 4). The
262 results confirm that the most relevant reactor section related to mass transfer is the sump,
263 where up to 3.30 $g \cdot min^{-1}$ of oxygen (335 mg O_2 L^{-1} h^{-1}) are desorbed during the daylight period,
264 while in the channel, a maximum value of 1.75 $g \cdot min^{-1}$ (7 mg O_2 L^{-1} h^{-1}) was determined. In the
265 paddlewheel, on the other hand, a maximum value of 1.50 $g \cdot min^{-1}$ (450 mg O_2 L^{-1} h^{-1}) is removed.
266 By applying Equation 8, it is possible to know not only the oxygen transfer capacity but also the
267 global mass transfer coefficients for the paddlewheel and the sump. The results show that the

268 global mass transfer coefficient values are stable throughout the day except at sunrise and
269 sunset, when the driving force approaches zero and the mass transfer coefficient values cannot
270 be determined (Figure 5). Considering the period from 12:00 to 17:00, when the driving force is
271 greatest, global mass transfer coefficient values of 49 and 34 h^{-1} are obtained for the
272 paddlewheel and the sump, respectively. This paddlewheel value is lower than that previously
273 reported, of 160 h^{-1} [2]; however, two different paddlewheel systems were used in each case
274 indicating that, although the paddlewheel is a standard impulsion system, modifications in its
275 design can affect the mass transfer capacity in this section of the reactor. Concerning the sump,
276 the global mass transfer coefficient determined was 34 h^{-1}, lower than the previously reported
277 value of 64 h^{-1} for the same air flow rate of 100 $L \cdot min^{-1}$ [2]; nonetheless, this was likewise due to
278 modifications in the diffuser system. In any case, the results show how the proposed
279 methodology can be used to estimate the global mass transfer coefficient value in an existing
280 raceway reactor without disturbing the reactor's normal operation. Consequently, the proposed
281 model can be used as a stable on-line sensor.

282 The utility of this methodology together with on-line sensors is the ability to measure any
283 variation in the mass transfer capacity as a function of the operational conditions, meaning that
284 one can make adjustments according to the system requirements. Given that liquid circulation
285 is not normally modified during raceway reactor operation, the global mass transfer coefficients
286 for the loop and the paddlewheel are constants; only the global mass transfer capacity in the
287 sump can be modified according to the gas flow rate supplied. To estimate this variation,
288 experiments were carried out on different days using the same methodology described
289 previously, but modifying the air flow rate in the sump from 50 to 350 $L \cdot min^{-1}$. Because the air
290 flow rate is not an intensive variable, it is a function of the total sump volume, correlating the
291 mass transfer coefficient with an intensive variable is preferred. Consequently, different
292 intensive variables can be used such as the power per unit of gas volume, the gas volume fraction
293 to total volume or hold-up, or the superficial gas velocity, amongst others [23]. In our case, the

294 superficial gas velocity was selected because it is easily calculated as the ratio between the gas
295 flow rate and the cross-sectional area of the sump, so additional measurements regarding
296 energy consumption or gas hold-up in the system are not required. The results show that the
297 mass transfer coefficient in the sump increased from 22 to 118 h^{-1} when the air flow rate
298 increased from 50 to 350 $L \cdot min^{-1}$, equivalent to variations in the superficial gas velocity from
299 0.0010 to 0.0073 $m \cdot s^{-1}$ (Figure 6). A potential relationship between both variables is therefore
300 obtained, with the exponent value less than one, indicating that with the higher superficial gas
301 velocity, the mass transfer coefficient will be saturated at its maximal value. In addition, because
302 this exponent was close to one, it indicates that the experiments were performed at low
303 superficial gas velocity values. Thus, in conventional mass transfer units such as bubble columns
304 or stirred reactors, the superficial gas velocity can reach values up to 0.12 $m \cdot s^{-1}$ [24]. Microalgae
305 reactors, on the other hand, have far lower superficial gas velocities, of up to 0.0015 $m \cdot s^{-1}$
306 [20,21], because microalgae cultures usually require lower mass transfer coefficients than
307 bacteria or yeast cultures. In any case, the correlation obtained (Equation 9) allows us to adjust
308 the mass transfer coefficient value by manipulating the superficial gas velocity, according to the
309 system requirements.

$$K_l a_{l,sump} = 10379 \cdot Ugr^{0.9123} \qquad \textit{Equation 9}$$

310 It is important to note that the supply of air imposes an additional energy consumption to liquid
311 circulation. Thus, in raceway reactors, the energy consumption for liquid circulation ranges from
312 1 to 10 $W \cdot m^{-3}$; in the case of the 100 m^2 raceway reactor used, a value of 4 $W \cdot m^{-3}$ was
313 determined, resulting in a net energy consumption of 1.9 kWh per day being measured. Air
314 supply from 50 to 350 $L \cdot min^{-1}$ imposes an additional energy consumption ranging from 0.6 to 4.0
315 kWh per day if maintaining the air flow constant throughout the day, thus increasing the energy
316 consumption from 29% to 200%. Previously, it was reported that the overall power consumption
317 in raceway reactors increases from 4 $W \cdot m^{-3}$ (1.9 kWh per day) when no gas is supplied to the
318 sump (only liquid circulation), up to 13 $W \cdot m^{-3}$ (6.2 kWh per day) when gas is supplied to the

sump at a maximum flow rate of 200 $m^3 h^{-1}$ [2]. Because photosynthesis take place mainly during the 6 h in the middle of the daylight period, the energy consumption for aeration can be reduced to a range from 0.2 to 1.3 kWh per day; this represents between 8 and 55% of energy consumption for liquid circulation. Numerous studies have demonstrated a wide range in the mass transfer coefficient values, between 0.4 and 350 h^{-1}, for various aerated systems [27]. In our study, the mass transfer coefficient values obtained in the sump agree with those reported previously for the same reactor [2] They are also similar to those previously reported for other types of microalgae reactors, such as 72 h^{-1} in rectangular airlift reactors [25], 22 h^{-1} in flat-panel reactors [26], and 108 h^{-1} in the airlift section of tubular photobioreactors [28]. Nevertheless, it is important to note that in rectangular or flat-panel reactors, the entire system is aerated so the mass transfer is taking place in the entire volume of the reactor. Conversely, with raceway reactors, as with tubular photobioreactors, the mass transfer mainly takes place in the aerated zones (the sump in raceway reactors and the bubble column/airlift system in tubular reactors) – so to compare the mass transfer coefficient in any kind of system, a value that considers the total reactor volume has to be used. Doing it this way, we see that in tubular reactors, the total mass transfer coefficient decreases to 10 h^{-1} [28], whereas in the raceway that we studied, the value ranged from 1.8 to 9.6 h^{-1}, a similar range of values to those in tubular reactors. These results confirm that the behaviour of raceway and tubular photobioreactors are not so different regarding mass transfer capacity, and that both systems must be carefully designed to meet the culture requirements with regard to their mass transfer capacity, especially in terms of oxygen desorption.

Finally, to evaluate the influence of the mass transfer capacity on the dissolved oxygen concentration at the end of the channel, simulations were performed using the experimental values for the oxygen production rate and the volumetric mass transfer coefficients in the different reactor sections (Figure 7). Data show that, if no air is supplied to the sump or if no sump exists in the reactor, the dissolved oxygen concentration in the culture can reach values

up 26 mg·L^{-1} (295 %Sat.) – these have been shown to dramatically reduce the performance of microalgae cultures [16,17]. When the mass transfer coefficient in the sump increases, the dissolved oxygen concentration decreases, but not in a linear fashion because the mass transfer capacity in the sump is limited. The dissolved oxygen concentration remains lower than 15 mg·L^{-1} (170 %Sat.) thus avoiding the negative effect of excessive concentration only when the mass transfer coefficient in the sump is higher than 50 h^{-1}; this means that the superficial gas velocity must be higher than 0.0003 m·s^{-1} and the air flow rate in the sump higher than 150 L·min^{-1}. A similar analysis can be performed when considering the variation in the oxygen production rate throughout the year, with the resultant difference in the required mass transfer capacity in the different seasons. The results show that the oxygen production rate in summer reaches values up to 6.8 g·min^{-1}, whereas in the winter, the maximal oxygen production rate is 1.63 g·min^{-1} (Figure 8). Differences in the oxygen production rate require different mass transfer coefficient values in the sump. To avoid oxygen accumulation above 15 mg·L^{-1} (thus ensuring there are no adverse effects from dissolved oxygen on the culture performance), the mass transfer coefficient in the sump must be higher than 70 h^{-1} in the summer, whereas in spring, the required value drops to 27 h^{-1} and in the autumn, to 15 h^{-1} (Figure 8). Only in winter is the oxygen production capacity so low that there is sufficient mass transfer in the channel and the paddlewheel to avoid dissolved oxygen accumulation above 15 mg·L^{-1}; making the required mass transfer coefficient value in the sump zero.

CONCLUSIONS

The mass transfer capacity in raceway reactors was studied. The results confirm that dissolved oxygen accumulation can limit biomass productivity in these systems if their mass transfer capacity is not optimized. Although oxygen is desorbed to the air in the channel and the paddlewheel, the sump is the reactor section that contributes most - therefore, the mass transfer capacity in this section must be optimized according to the oxygen production rate in the system. The influence of gas flow on the mass transfer coefficient was also determined,

obtaining a calibrated empirical model. Using this model, it is possible to properly regulate the air flow in the sump so that the reactor operation can be optimized. The methodology proposed allows us to determine and then optimize the mass transfer capacity in the sump of any raceway reactor. For this reason, it is a powerful tool for the optimization of existing reactors as well as in optimizing the design of new reactors.

Acknowledgements

This study was supported financially by the Ministry of Economy and Competitiveness (DPI2014-55932-C2-1-R, DPI2017-84259-C2-1-R) and (EDARSOL, CTQ2014-57293-C3-1-R), and the European Union's Horizon 2020 Research and Innovation Program under Grant Agreement No. 727874 SABANA. We are most grateful for the practical assistance given by the staff of the Cajamar Foundation's "Las Palmerillas" Experimental Station. We are also grateful to Daniel Algarra Navas for his work on the graphical design of **¡Error! No se encuentra el origen de la referencia.**.

Author contributions statement

M. Barceló-Villalobos was responsible for the work and data collection, in addition to writing the manuscript. J. L. Guzmán Sánchez was responsible for data processing and contributed to the elaboration of the manuscript. I. Martín Cara was responsible for the operation of the reactors and verifying the data quality. J.A. Sánchez Molina was responsible for developing the models. F. G. Acién Fernández was responsible for the team and coordinating the work, mainly participating in the discussion regarding the results and finalizing the manuscript.

Conflict of interest statement

The authors declare no potential financial or other interests that could be perceived as influencing the outcome of the research.

Statement of Informed Consent, Human/Animal Rights

“No conflicts, informed consent, human or animal rights are applicable”

Declaration of authors

All the participants share authorship of this work and agree to submit the manuscript for peer review to Algal Research.

References

[1] J. Benemann, Microalgae for biofuels and animal feeds, Energies. 6 (2013) 5869–5886.

[2] J.L. Mendoza, M.R. Granados, I. de Godos, F.G. Acién, E. Molina, S. Heaven, C.J. Banks, Oxygen transfer and evolution in microalgal culture in open raceways, Bioresour. Technol. 137 (2013) 188–195.

[3] S. Li, S. Luo, R. Guo, Efficiency of CO2 fixation by microalgae in a closed raceway pond, Bioresour. Technol. 136 (2013) 267–272.

[4] I. de Godos, J.L. Mendoza, F.G. Acién, E. Molina, C.J. Banks, S. Heaven, F. Rogalla, Evaluation of carbon dioxide mass transfer in raceway reactors for microalgae culture using flue gases, Bioresour. Technol. 153 (2014) 307–314. doi:10.1016/j.biortech.2013.11.087.

[5] A. Pawlowski, I. Fernández, J.L.L. Guzmán, M. Berenguel, F.G.G. Acién, J.E.E. Normey-Rico, Event-based predictive control of pH in tubular photobioreactors, Comput. Chem. Eng. 65 (2014) 28–39. doi:10.1016/j.compchemeng.2014.03.001.

[6] D. Ippoliti, A. González, I. Martín, J.M.F. Sevilla, R. Pistocchi, F.G. Acién, Outdoor production of Tisochrysis lutea in pilot-scale tubular photobioreactors, J. Appl. Phycol. 28 (2016) 3159–3166. doi:10.1007/s10811-016-0856-x.

[7] Y. Bao, M. Liu, X. Wu, W. Cong, Z. Ning, In situ carbon supplementation in large-scale cultivations of Spirulina platensis in open raceway pond, Biotechnol. Bioprocess Eng. 17

418 (2012) 93–99.

419 [8] E. Posadas, M.M. Morales, C. Gomez, F.G. Acién, R. Muñoz, Influence of pH and CO2
420 source on the performance of microalgae-based secondary domestic wastewater
421 treatment in outdoors pilot raceways, Chem. Eng. J. 265 (2015) 239–248.

422 [9] C. Jiménez, B.R. Cossío, D. Labella, F.X. Niell, The feasibility of industrial production of
423 Spirulina (Arthrospira) in Southern Spain, Aquaculture. 217 (2003) 179–190.
424 doi:10.1016/S0044-8486(02)00118-7.

425 [10] I. de Godos, J.L. Mendoza, F.G. Acién, E. Molina, C.J. Banks, S. Heaven, F. Rogalla,
426 Evaluation of carbon dioxide mass transfer in raceway reactors for microalgae culture
427 using flue gases, Bioresour. Technol. 153 (2014) 307–314.
428 doi:10.1016/j.biortech.2013.11.087.

429 [11] S.C. James, V. Boriah, Modeling algae growth in an open-channel raceway, J. Comput.
430 Biol. 17 (2010) 895–906.

431 [12] Y.H. Wang, R. Turton, K. Semmens, T. Borisova, Raceway design and simulation system
432 (RDSS): An event-based program to simulate the day-to-day operations of multiple-tank
433 raceways, Aquac. Eng. 39 (2008) 59–71. doi:10.1016/j.aquaeng.2008.06.002.

434 [13] J.L. Mendoza, M.R. Granados, I. de Godos, F.G. Acién, E. Molina, C. Banks, S. Heaven,
435 Fluid-dynamic characterization of real-scale raceway reactors for microalgae production,
436 Biomass and Bioenergy. 54 (2013) 267–275. doi:10.1016/j.biombioe.2013.03.017.

437 [14] K. Sompech, Y. Chisti, T. Srinophakun, Design of raceway ponds for producing microalgae,
438 Biofuels. 3 (2012) 387–397.

439 [15] I. Fernández, F.G. Acién, J.M. Fernández, J.L. Guzmán, J.J. Magán, M. Berenguel, Dynamic
440 model of microalgal production in tubular photobioreactors, Bioresour. Technol. 126
441 (2012) 172–181. doi:10.1016/j.biortech.2012.08.087.

[16] A. Pawlowski, J.L. Mendoza, J.L. Guzmán, M. Berenguel, F.G. Acién, S. Dormido, Effective utilization of flue gases in raceway reactor with event-based pH control for microalgae culture, Bioresour. Technol. 170 (2014) 1–9. doi:10.1016/j.biortech.2014.07.088.

[17] I. Fernández, F.G. Acién, J.L. Guzmán, M. Berenguel, J.L. Mendoza, Dynamic model of an industrial raceway reactor for microalgae production, Algal Res. 17 (2016) 67–78. doi:10.1016/j.algal.2016.04.021

[18] A.S. Mirón, A.C. Gómez, F.G. Camacho, E.M. Grima, Y. Chisti, Comparative evaluation of compact photobioreactors for large-scale monoculture of microalgae, Prog. Ind. Microbiol. 35 (1999) 249–270. doi:10.1016/S0079-6352(99)80119-2.

[19] C. Sousa, D. Valev, M.H. Vermuë, R.H. Wijffels, Effect of dynamic oxygen concentrations on the growth of Neochloris oleoabundans at sub-saturating light conditions, Bioresour. Technol. 142 (2013). doi:10.1016/j.biortech.2013.05.041.

[20] T.A.A. Costache, F.G.A. Fernández, F.G. Acien, M.M. Morales, J.M. Fernández-Sevilla, I. Stamatin, E. Molina, Comprehensive model of microalgae photosynthesis rate as a function of culture conditions in photobioreactors, Appl. Microbiol. Biotechnol. 97 (2013) 7627–7637.

[21] D. Ippoliti, C. Gómez, M.M. Morales-Amaral, R. Pistocchi, J.M.M. Fernández-Sevilla, F.G.G. Acién, Modeling of photosynthesis and respiration rate for Isochrysis galbana (T-Iso) and its influence on the production of this strain, Bioresour. Technol. 203 (2016) 71–79.

[22] R.W. Babcock, A. Wellbrock, P. Slenders, J.A.C. Radway, Improving mass transfer in an inclined tubular photobioreactor, (2015) 1–9. doi:10.1007/s10811-015-0763-6.

[23] F. Garcia-Ochoa, E. Gomez, Bioreactor scale-up and oxygen transfer rate in microbial processes: An overview, Biotechnol. Adv. 27 (2009) 153–176.

466 doi:10.1016/j.biotechadv.2008.10.006.

467 [24] Y. Chisti, U.J. Jauregui-Haza, Oxygen transfer and mixing in mechanically agitated airlift
468 bioreactors, Biochem. Eng. J. 10 (2002) 143–153.

469 [25] X. Guo, L. Yao, Q. Huang, Aeration and mass transfer optimization in a rectangular airlift
470 loop photobioreactor for the production of microalgae, Bioresour. Technol. 190 (2015)
471 189–195. doi:10.1016/j.biortech.2015.04.077.

472 [26] E. Sierra, F.G. Acién, J.M. Fernández, J.L. García, C. González, E. Molina, Characterization
473 of a flat plate photobioreactor for the production of microalgae, Chem. Eng. J. 138 (2008)
474 136–147.

475 [27] A.P. Carvalho, L.A. Meireles, F.X. Malcata, Microalgal reactors: A review of enclosed
476 system designs and performances, Biotechnol. Prog. 22 (2006) 1490–1506.

477 [28] F. Camacho-Rubio, F.G. Acién, J.A. Sánchez-Pérez, F. García-Camacho, E. Molina-Grima,
478 Prediction of dissolved oxygen and carbon dioxide concentration profiles in tubular
479 photobioreactors for microalgal culture, Biotechnol. Bioeng. 62 (1999) 71–86.
480 doi:10.1002/(SICI)1097-0290(19990105)62:1<71::AID-BIT9>3.0.CO;2-T.

481

482 Nomenclature:

Variable	Units	Description
PO_2	$g \cdot min^{-1}$	Oxygen production by photosynthesis
NO_2	$g \cdot min^{-1}$	Oxygen transfer between the culture and the air
K_la_l	min^{-1}	Volumetric mass transfer coefficient
$[O_2]$	$mg \cdot L^{-1}$	Dissolved oxygen concentration
$[O_{2*}]$	$mg \cdot L^{-1}$	Dissolved oxygen concentration in equilibrium with air

V	L	Volume of the respective zone
T	ºC	Temperature of the culture
Q_{liquid}	$L \cdot min^{-1}$	Liquid flow rate
Ugr	$m \cdot s^{-1}$	Superficial gas velocity

483

484

485 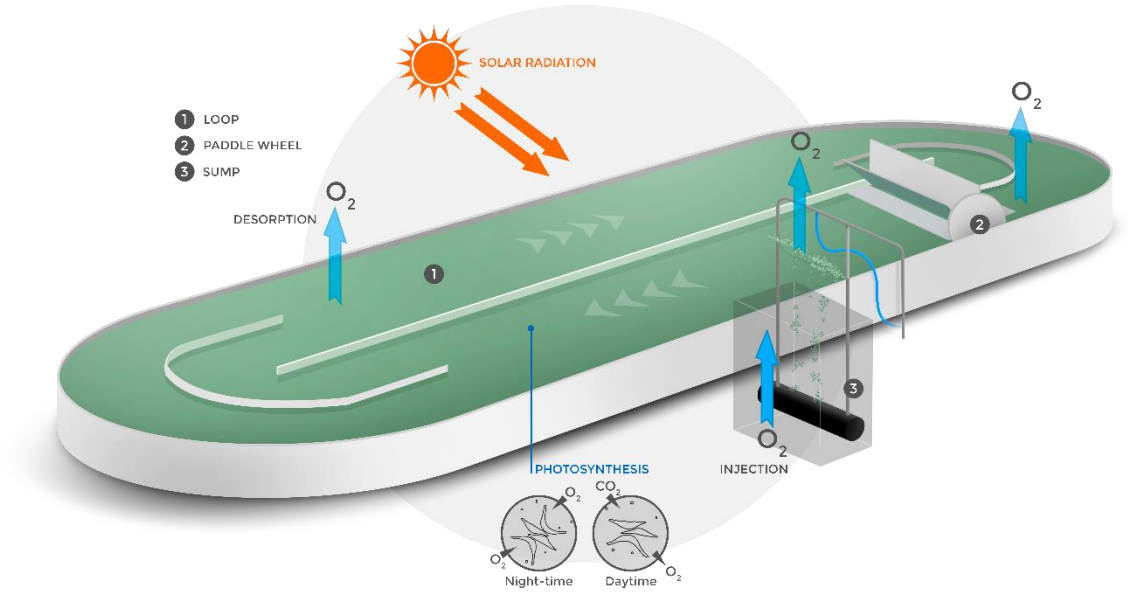

486 *Figure 1.- Scheme of the 100 m^2 raceway reactor used to study this type of system and the mass*
487 *transfer capacity, indicating the major phenomena taking place.*

488

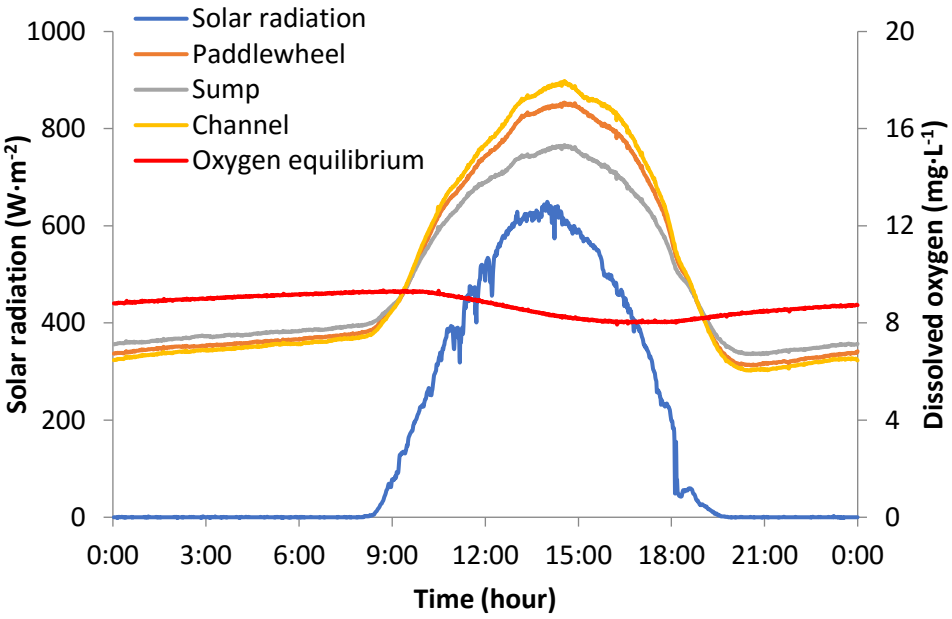

489

490 *Figure 2.- Daily variation in solar radiation and dissolved oxygen concentration at the different*
491 *positions in the reactor.*

492

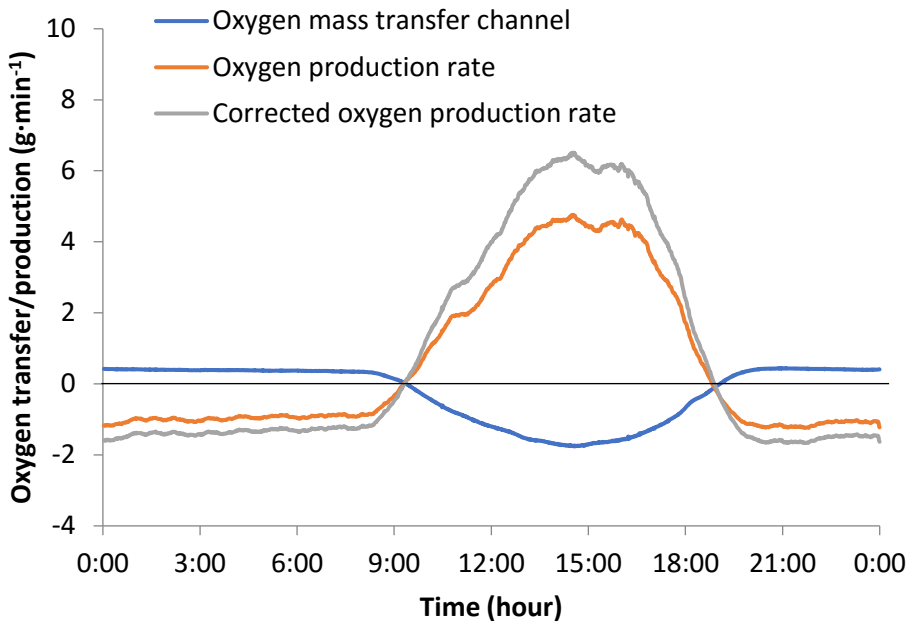

493

494 *Figure 3.- Daily oxygen transfer variation in the loop and oxygen production in the reactor;*
495 *estimated from data on dissolved oxygen concentration at the beginning and end of the channel*
496 *using Equation 5.*

497

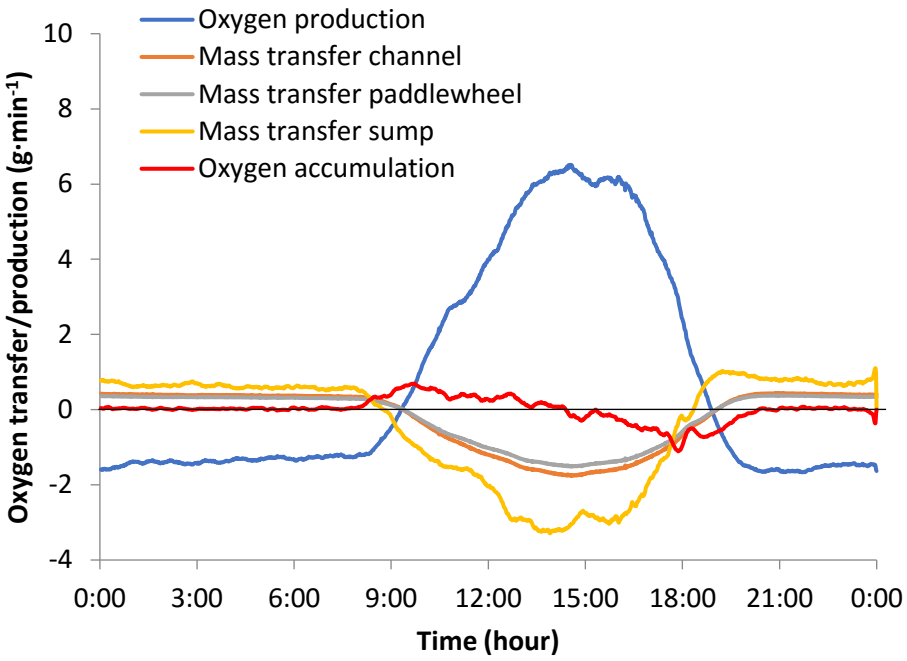

498

499 *Figure 4.- Daily variation in oxygen production, oxygen transfer in each raceway reactor section*
500 *and oxygen accumulation in the reactor; estimated from data on dissolved oxygen concentration*
501 *at the different positions using Equation 6.*

502

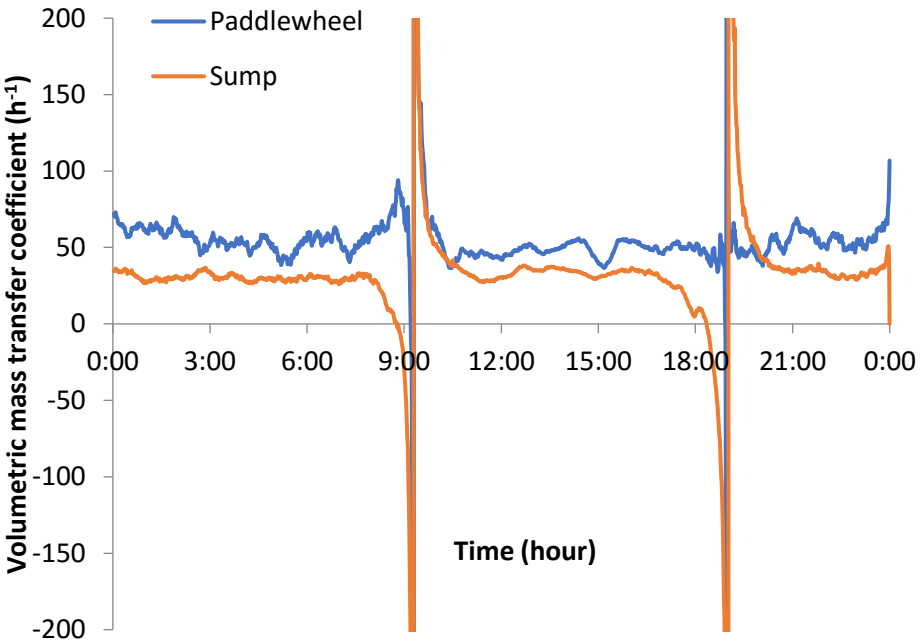

503

504 *Figure 5.- Daily variation in the volumetric mass transfer coefficient in the paddlewheel and*
505 *sump.*

506

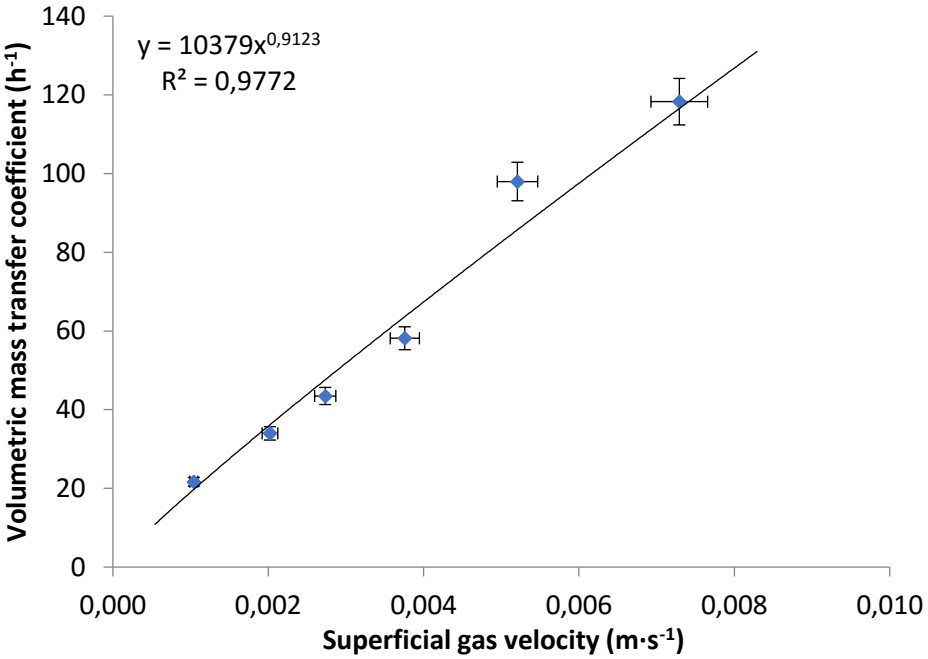

507

508 *Figure 6.- Variation in the mass transfer coefficient in the sump as a function of the air flow rate,*
509 *expressed as the superficial gas velocity. Values obtained using the proposed methodology to*
510 *estimate the mass transfer coefficient in raceway reactors. Data shown as mean ± SD, n=31.*

511

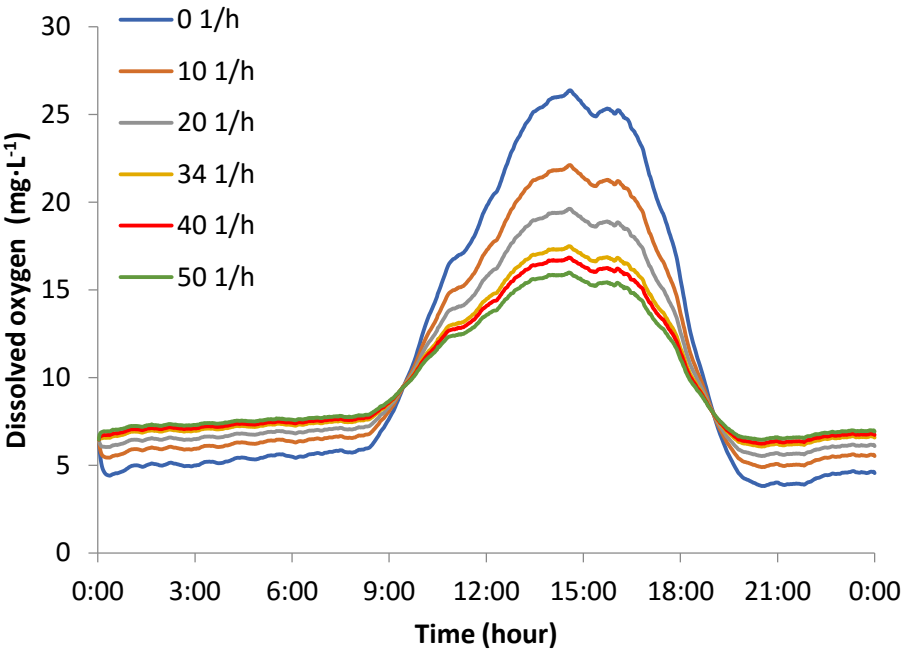

512

513 *Figure 7.- Variation in the dissolved oxygen concentration at the end of the channel as a function*
514 *of the volumetric mass transfer coefficient in the sump. Values obtained using experimental*
515 *measurements for the oxygen production rate and simulating the mass transfer capacity in the*
516 *different reactor sections according to the reported values for the volumetric mass transfer*
517 *coefficients.*

518

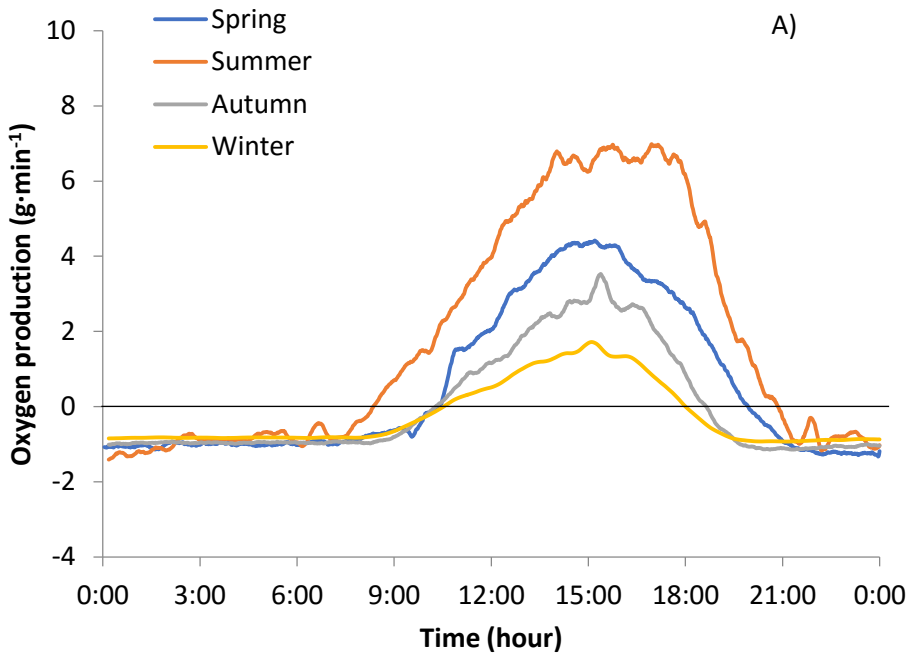

519

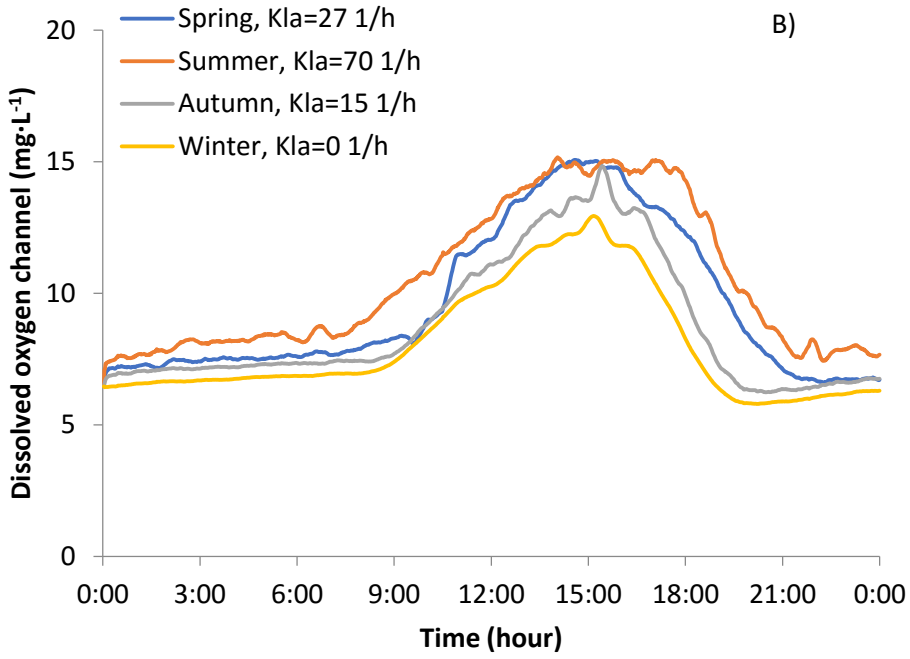

520

521 *Figure 8.- (A) Daily variation in the oxygen production rate during the different seasons of the*
522 *year; (B) Mass transfer coefficient values in the sump required to avoid oxygen accumulation*
523 *above 15 mg·L^{-1} according to the methodology proposed.*

524